Optimal Distributed Allocation of Almost Blank Subframes for LTE/WiFi Coexistence

Shubhajeet Chatterjee, Mohammad J. Abdel-Rahman and Allen B. MacKenzie
Electrical and Computer Engineering Department, Virginia Tech, USA
{shubh92, mo7ammad, mackenab}@vt.edu

***Abstract*—Since LTE in unlicensed spectrum (LTE-U) was proposed by Qualcomm, it has drawn considerable interest because of its potential to increase the capacity of existing LTE networks by utilizing existing infrastructure in the unlicensed band. But, Wi-Fi technology, already operating in the unlicensed 5 GHz band, creates several potential challenges for managing the activities of these two different technologies in the same band.**

In this context, we propose an adaptive coexistence scheme between LTE and WiFi by utilizing almost blank subframes (ABS). An ABS is an LTE subframe of duration 1 ms (containing two time slots of 0.5 ms duration) with reduced downlink activity. LTE allocates ABSs over 20 MHz channels in 5 GHz band to allow WiFi to access the spectrum. In the proposed coexistence scheme, each LTE cell optimally distributes ABSs over the frame to provide certain quality of service (QoS) guarantees for WiFi traffic while ensuring the performance of its own users.

***Index Terms*—LTE/WiFi coexistence, almost blank subframes (ABSs), quorum systems, integer programming.**

I. Introduction

When LTE and WiFi share spectrum, unfairness arises due to their different channel access mechanisms. For channel access, WiFi follows a carrier sense multiple access with collision avoidance (CSMA/CA) protocol where each WiFi transmitter senses the channel energy for a transmission opportunity, i.e. listen before talk (LBT) with a random backoff time. For LTE, each eNodeB (eNB) allocates frequencies and time slots to user equipment (UE) in a centralized fashion. Due to these different channel access mechanisms of LTE and WiFi (i.e. centralized and decentralized), it is likely that LTE would dominate WiFi in the 5 GHz band [1], [2]. Therefore, an efficient coexistence protocol is needed to be enable for fair and harmonious spectrum sharing between these two technologies.

In search of harmonious coexistence, research has taken two approaches: LBT-based solutions (where LTE also performs LBT before accessing the channels [3]–[5]) and channel sensing (CS)-based solutions (where LTE senses the channel periodically and based on the sensed information about channel activity, takes action in the power domain [6]–[8] or in the frequency domain [7]–[11] or in the time domain [9], [10], [12]–[16]). Compared to LBT, CS-based schemes have gained popularity because they do not require any changes to existing LTE protocols. Also, 3GPP had not yet standardized LBT for LTE-U.

In this paper, we propose an ABS-based (time-domain) CS scheme. ABSs were introduced in LTE Release-10 by 3GPP. The term 'Almost Blank' signifies the presence of some channel information (e.g. channel estimation, radio resource management) in this subframe without any data. Although authors of [9], [13], [17] already proposed coexistence schemes based on static and adaptive ABS allocation, their focus was limited to decide the number of ABSs. Once the number of ABSs is decided, the first subframes of the frame are designated as ABSs, as shown in Figures 1(a) and 1(b). This produces satisfactory results for WiFi throughput in a single LTE cell (in the rest of this paper we will use the term 'cell' to denote LTE cells) with WiFi network coexistence. But, in the case of an LTE network consisting of multiple overlapping LTE cells, WiFi users lying in the overlapping region of two or more different cells, will not be able to access the spectrum if the ABSs of the two neighboring cells are not synchronized, as shown in Figure 1(b). One simple solution is to synchronize the LTE frames and allocate ABSs in standardized locations in each frame, but this solution has multiple drawbacks. First, achieving frame-level synchronization (in milliseconds) is potentially challenging, especially when the cells are operated by different operators. Furthermore, each ABS causes 1 ms delay for the LTE traffic. Even if the cell-edge WiFi accessibility problem is solved, sequentially allocating n consecutive ABSs will result in an n ms delay for the LTE users (shown in Figure 1(a)), resulting in a rapid degradation in LTE performance. For example, when the number of ABSs in both cells is large (say 7 or 8 ABSs out of 10 subframes), sequential ABS allocation may result in some overlapped ABSs but the delay to LTE users will be increased to 7 ms or 8 ms.

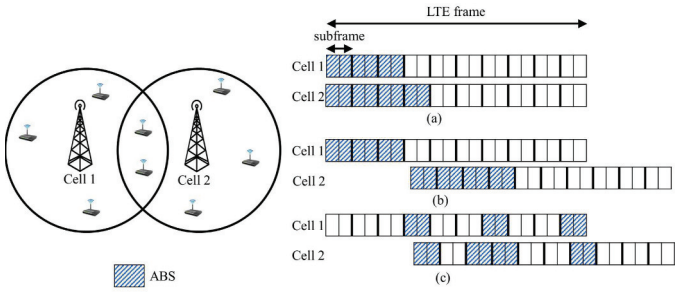

Fig. 1: Issues with cell edge users.

In this paper, we develop an adaptive and distributed ABS allocation scheme that maximizes the accessibility of the spec-

978-3-901882-90-6/17 ©2017 IFIP

trum for all WiFi users (i.e. including cell-edge users), while minimizing the delay for LTE users as shown in Figure 1(c).

Quorum systems were developed to aid in synchronization of operations in distributed systems. Informally, a quorum system is subsets of a given set where each pair of subsets has a non-empty intersection. Here, we apply this distributed design strategy and non-empty intersection property of quorum systems to design an efficient ABS allocation scheme.

Our Contributions– Based on channel sensing, for a given number of ABSs, we aim to develop an adaptive and distributed ABS allocation scheme that can provide certain QoS guarantees for both WiFi and LTE technologies. Towards achieving this goal, we develop a decentralized multi-objective sequential optimization framework over combinatorics to generate ABS location sets which satisfy certain QoS requirements of both networks, i.e. *maximizes* the throughput for cell-edge WiFi users and *minimizes* the delay for LTE users. This framework can be applied to achieve synchronization in other time domain and frequency domain coexistence schemes with simple modifications. Further, new constraints can be added in this optimization framework (e.g. to support channel bonding for WiFi) to enhance the performance of the scheme.

Paper Organization–The rest of the paper is organized as follows. Section II describes the system model. Section III presents basic design principle for quorum systems. Section IV explains the optimal ABS allocation scheme. The numerical analysis is presented and discussed in Section V. Finally the paper is concluded in Section VI.

II. System Model

We consider an LTE network that is divided into a set $\mathcal{U} \overset{\text{def}}{=} \{1, 2, \ldots, U\}$ of small cells. Suppose that the timing misalignment between the LTE frames of cell i and j (where $i, j \in \mathcal{U}$ and $i \neq j$) is τ_{ij}. Let, cell i senses the WiFi activity (based on WiFi preambles) over the spectrum and assigns n_i subframes of an LTE frame (which contains 9 subframes) as ABSs. Subsequently, WiFi activity can only be measured during ABSs, as WiFi can access the spectrum only during the ABSs. The implementation of an efficient estimation scheme to decide the number of ABSs is beyond the scope of this paper. As backward compatibility is not required for LTE in 5 GHz band, assume that ABSs are completely vacated to reduce the interference for WiFi, similar to the previous ABS-based coexistence schemes [9], [13], [17]. Our goal is to develop a distributed and optimal ABS allocation scheme, such that each cell i independently allocates their n_i ABSs in a frame such that:

- For each neighbor cell j of i, the accessibility of ABSs for the cell-edge WiFi users of i and j is maximized.
- Delay of LTE users in i is minimized.

III. Background and Basic Design

A. Preliminaries

Here, we describe the basic idea of a quorum system and its properties.

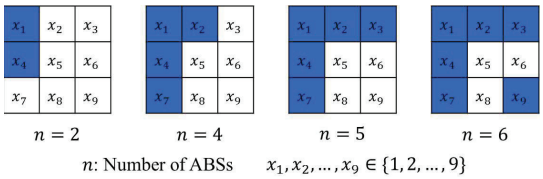

Fig. 2: ABS allocation technique from a grid quorum system.

Definition 1: Given a set of non-negative integers $Z_n = 0, 1, \ldots, n-1$, a quorum system Q under Z_n is a collection of non-empty subsets of Z_n, each called a quorum, such that $\forall G\ ,\ H \in Q,\ G \bigcap H \neq \emptyset$.

Definition 2: Given a non-negative integer i and a quorum G in a quorum system Q under Z_n, we define rotate $(G, i) = \{(x + i) \mod n, x \in G\}$ as a cyclic rotation of G by i.

Definition 3: A quorum system Q under Z_n satisfies the rotation closure property if $\forall G_1, G_2 \in Q$ and $\forall i_1, i_2 \in Z_n$, $\text{rotate}(G_1, i_1) \cap \text{rotate}(G_2, i_2) \neq \emptyset$.

Throughout the paper, Z_n is used to denote the set of non-negative integers less than n. Quorum systems that satisfy rotation closure property (e.g. grid quorum) can be applied to achieve overlapped ABSs among different cells.

Definition 4: A grid quorum system arranges the elements of Z_n as $\sqrt{n} \times \sqrt{n}$ grid, where n needs to be the square of a positive integer. A quorum is a complete row and column of the grid. So, the size of a quorum in grid quorum system is $2\sqrt{n} - 1$.

B. Basic Design

Utilizing the idea of grid quorum i.e. creating sets by selecting elements from the rows and columns of a square grid to satisfy rotation closure property and non-empty intersection property, in this section we develop a distributed ABS allocation scheme. First, let us consider the 9 subframes of a frame to be numbered as $1, 2, \ldots, 9$ and denote them as set $\mathcal{S}$. $\mathcal{S}$ generates a square grid x_s, $s \in \mathcal{S}$, of size 3×3 as shown in Figure 2. Each i independently generates such square grids and decides the locations of n_i ABSs from the square grid $x_s, s \in \mathcal{S}$, by following Algorithm 1 for distributed ABS allocation. This ABS location selection process is further explained in Figure 2.

Now, let us consider a particular grid structure $x_s, s \in \mathcal{S}$, where $x_1 = 1, x_2 = 2, \ldots, x_9 = 9$ as shown in Figure 3. For $n_i = 2\sqrt{9} - 1 = 5$ and $n_j = 5$, the ABS location sets of i and j selected from this grid following our algorithm result in complete quorum (as discussed in subsection III-A). So, these ABS location sets satisfy rotation closure property and non-empty intersection property of the grid quorums. Thus cell i and j will have at least two overlapped ABSs irrespective of their frame timings. If the subframes are also misaligned, then, due to cyclic rotation of the LTE frames, at least half of two ABSs will overlap irrespective of the timing misalignment of the subframes, as shown in Figure 3. So, for $n_i = n_j = 5$, this particular grid structure *guarantees* the availability of at least one ABS (half of two ABSs) for the WiFi users in the overlapped cell edges of i and j.

Algorithm 1 Distributed ABS Allocation

if $n_i < 3$ **then**
  a row or a column is randomly selected
  if row is selected **then**
    n_i elements from the left end of the row are selected
  else
    n_i elements from the top of the column are selected
  end if
end if
if $n_i = 4$ **then**
  All the elements from a row *or* a column are randomly selected and 1 element is selected from the adjacent row or column
end if
if $n_i = 5$ **then**
  All the elements from a randomly picked row *and* a randomly picked column are selected.
end if
if $n_i > 5$ **then**
  All the elements from a randomly picked row *and* a randomly picked column are selected and $n_i - 5$ elements are randomly selected.
end if

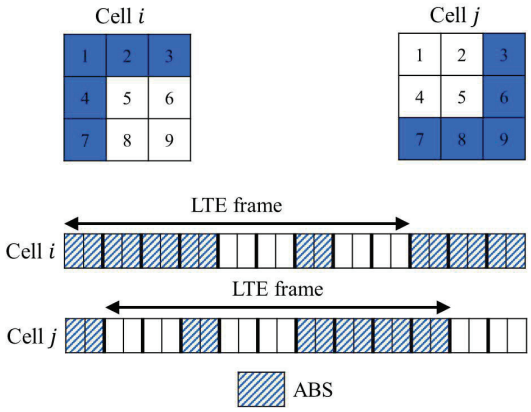

Fig. 3: Guaranteed overlap for $n_i = 5$ and $n_j = 5$.

But, if $n_i < 5$ or $n_j < 5$, we cannot guarantee any overlapped ABS in this grid structure. Also, the ABS location sets selected from this particular square grid, results 4 consecutive ABSs, resulting delay of 4 ms for LTE users.

Now, this square grid is one of the $9! = 362880$ square grid structures that can be generated from set $\mathcal{S}$. ABS location sets selected from different grid structures would result in different numbers of overlapped ABSs and different numbers of consecutive ABSs. So, in the next section we develop two multi-objective sequential optimization frameworks to optimally design the square grid $x_s, s \in \mathcal{S}$, to achieve certain probabilistic QoS guarantees for both the WiFi and LTE networks.

IV. Optimal ABS Allocation

In our distributed ABS allocation scheme, cell i selects the locations of the n_i ABSs from a square grid of $x_s, s \in \mathcal{S}$. Let $\mathcal{R}(x_s, n_i, \tilde{n}_j, \tilde{\tau}_{ij})$ be the number of overlapped ABSs with cell j and let $\mathcal{D}(x_s, n_i, \tilde{n}_j, \tilde{\tau}_{ij})$ be the number of consecutive ABSs in cell i, where $\tilde{n}_j \in \mathcal{S}$ and $\tilde{\tau}_{ij} \in Z_9$. Based on our design goal, maximizing $\mathcal{R}$ will improve the average throughput of cell-edge WiFi users and minimizing $\mathcal{D}$ would reduce the average delay of LTE. We can readily assume that the distributions of $\tilde{n}_j$ and $\tilde{\tau}_{ij}$ are independent of each other as the number of ABSs of a cell does not depend on frame time misalignment with the neighbor cells.

Now, let us formulate the multi-objective sequential optimization problem for optimizing the grid structure for cell i that improves the performance of cell-edge WiFi network without significantly increasing the delay of LTE network, for given distributions of $\tilde{n}_j$ and $\tilde{\tau}_{ij}$, as follows:

Problem 1: Optimal ABS Allocation

Stage 1:

$$\underset{\{x_s, s\in\mathcal{S}\}}{\text{maximize}} \left\{ \sum_{a=1}^{9} \sum_{b=0}^{8} \Big[\mathcal{R}(x_s, n_i, \tilde{n}_j = a, \tilde{\tau}_{ij} = b) \times \Pr(\tilde{n}_j = a) \Pr(\tilde{\tau}_{ij} = b) \Big] \right\} \quad (1)$$

subject to:

$$x_s \in \{1, 2, \ldots, 9\}$$

Stage 2:

$$\underset{\{x_s, s\in\mathcal{S}\}}{\text{minimize}} \left\{ \sum_{a=1}^{9} \sum_{b=0}^{8} \Big[\mathcal{D}(x_s, n_i, \tilde{n}_j = a, \tilde{\tau}_{ij} = b) \times \Pr(\tilde{n}_j = a) \Pr(\tilde{\tau}_{ij} = b) \Big] \right\} \quad (2)$$

subject to:

$$\left\{ \sum_{a=1}^{9} \sum_{b=0}^{8} \Big[\mathcal{R}(x_s, n_i, \tilde{n}_j = a, \tilde{\tau}_{ij} = b) \Pr(\tilde{n}_j = a) \times \Pr(\tilde{\tau}_{ij} = b) \Big] \right\} \geq (1-\epsilon) \left\{ \sum_{a=1}^{9} \sum_{b=0}^{8} \Big[\mathcal{R}(x_s^*, n_i, \tilde{n}_j = a, \tilde{\tau}_{ij} = b) \times \Pr(\tilde{n}_j = a) \Pr(\tilde{\tau}_{ij} = b) \Big] \right\} \quad (3)$$

$$(x_s, x_s^*) \in \{1, 2, \ldots, 9\}.$$

In this optimization problem, x_s^*, $s \in \mathcal{S}$, denotes the optimal solution (i.e. the optimal square grid structure) for the problem at Stage 1, i.e. (1). Keeping this solution as constraint (3), opti-

mal solution for Stage 2, i.e. (2) is obtained for different values of ϵ, where $0 \leq \epsilon \leq 1$. If $\epsilon = 0$, from (3), the purpose of Stage 2 is to select from the first-stage optimal solutions (if there are multiple) the one that minimizes $\mathcal{D}\left(x_s, n_i, \tilde{n}_j = a, \tilde{\tau}_{ij} = b\right)$, i.e. the number of consecutive ABSs. If $\epsilon > 0$, then Stage 2 aims to minimize $\mathcal{D}\left(x_s, n_i, \tilde{n}_j = a, \tilde{\tau}_{ij} = b\right)$ without reducing the value of $\mathcal{R}\left(x_s, n_i, \tilde{n}_j = a, \tilde{\tau}_{ij} = b\right)$ by more than ϵ fraction of its optimal value (obtained from Stage 1). The larger the value of ϵ, the more impact the number of non-consecutive ABSs has on the allocation decision.

Similar to Problem 1, we can formulate another sequential optimization problem to ensure minimum delay for the LTE network without significantly degrading the performance of the cell-edge WiFi network, as shown in Problem 2.

Problem 2: Optimal ABS Allocation

STAGE 1:

$$\underset{\{x_s, s\in\mathcal{S}\}}{\text{minimize}} \left\{ \sum_{a=1}^{9} \sum_{b=0}^{8} \left[\mathcal{D}\left(x_s, n_i, \tilde{n}_j = a, \tilde{\tau}_{ij} = b\right) \times \Pr\left(\tilde{n}_j = a\right) \Pr\left(\tilde{\tau}_{ij} = b\right) \right] \right\} \quad (4)$$

subject to:

$x_s \in \{1, 2, \ldots, 9\}$

STAGE 2:

$$\underset{\{x_s, s\in\mathcal{S}\}}{\text{maximize}} \left\{ \sum_{a=1}^{9} \sum_{b=0}^{8} \left[\mathcal{R}\left(x_s, n_i, \tilde{n}_j = a, \tilde{\tau}_{ij} = b\right) \times \Pr\left(\tilde{n}_j = a\right) \Pr\left(\tilde{\tau}_{ij} = b\right) \right] \right\} \quad (5)$$

subject to:

$$\left\{ \sum_{a=1}^{9} \sum_{b=0}^{8} \left[\mathcal{D}\left(x_s, n_i, \tilde{n}_j = a, \tilde{\tau}_{ij} = b\right) \Pr\left(\tilde{n}_j = a\right) \times \Pr\left(\tilde{\tau}_{ij} = b\right) \right] \right\} \geq (1-\epsilon) \left\{ \sum_{a=1}^{9} \sum_{b=0}^{8} \left[\mathcal{D}\left(x_s^*, n_i, \tilde{n}_j = a, \tilde{\tau}_{ij} = b\right) \times \Pr\left(\tilde{n}_j = a\right) \Pr\left(\tilde{\tau}_{ij} = b\right) \right] \right\} \quad (6)$$

$(x_s, x_s^*) \in \{1, 2, \ldots, 9\}$.

The optimization parameters $\mathcal{R}\left(x_s, n_i, \tilde{n}_j, \tilde{\tau}_{ij}\right)$ and $\mathcal{D}\left(x_s, n_i, \tilde{n}_j, \tilde{\tau}_{ij}\right)$ cannot be expressed as closed-form expressions because they produce different set of results for different grid structures i.e. $x_s, s \in \mathcal{S}$. So, the optimization problems can not be solved numerically. We solved these problems by running exhaustive search algorithms in MATLAB scripts.

TABLE I: Simulation Parameters

Parameters	Settings
DIFS	34 μs
SIFS	16 μs
Slot Durations (σ)	9 μs
Average Frame Transmission time(T_{FRA})	15 ms
Average Acknowledgment time(T_{ACK})	10 ms
Min. Backoff Window	16
Max. Backoff Window	1024
Min. Backoff stage	6
WiFi Channel Bit Rate (S_j)	128 Mbps
Number of cell-edge WiFi users (w)	200

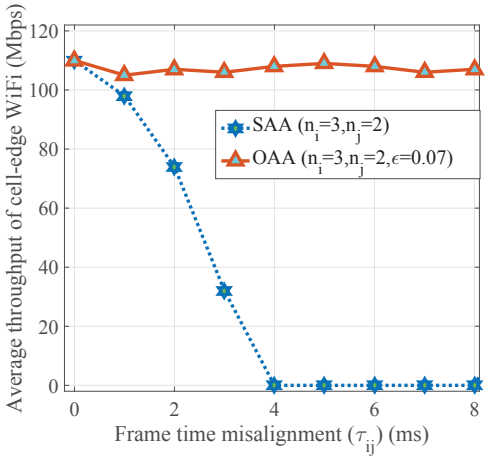

Fig. 4: Average throughput of cell-edge WiFi network vs. frame time misalignment (τ_{ij}) (Problem 1).

V. NUMERICAL EVALUATION

In this section, we evaluate the solution of Problems 1 and 2 for different values of n_i, n_j, τ_{ij}, and ϵ. All numerical analysis are performed in MATLAB. To solve the optimization problems of cell i (or j), we consider uniform distributions for $\tilde{n}_j$ (or $\tilde{n_i}$) and $\tilde{\tau}_{ij}$ (or $\tilde{\tau}_{ji}$). The simulation parameters are shown in Table 1.

As the minimum and maximum backoff window sizes of the WiFi network are 16 and 1024 respectively, for our simulation purpose, we consider the transmission probabilities of WiFi users (i.e. p_i and p_j in (7)) to be chosen randomly from the set $\left\{1, \frac{1}{16}, \frac{1}{17}, \frac{1}{18}, \ldots, \frac{1}{1024}\right\}$.

We compare our Optimal ABS Allocation (OAA) scheme with the Sequential ABS Allocation (SAA) scheme adopted in [9], [13], [17]. For the optimal solution x_s^* and a given set of parameters n_i, n_j, and τ_{ij}, the average throughput of the WiFi network can be expressed as follows [18]:

$$s_{\text{WiFi}} = \frac{1}{w} \mathcal{R}\left(x_s^*, n_i, n_j, \tau_{ij}\right) \sum_{i=1}^{w} \frac{p_j p_e S_j}{\sigma p_e + T_b\left(1 - p_e\right)}, \quad (7)$$

where $p_e = \prod_{i=1, i\neq j}^{w} \left(1 - p_i\right)$ and $T_b = (T_{\text{FRA}} + SIFS + T_{\text{ACK}}$. The delay of the LTE network is given be $\mathcal{D}\left(x_s^*, n_i, n_j, \tau_{ij}\right)$.

First, in Figures 4 and 5, we evaluate the performance of the optimal solution of Problem 1 by varying τ_{ij} from 0 ms

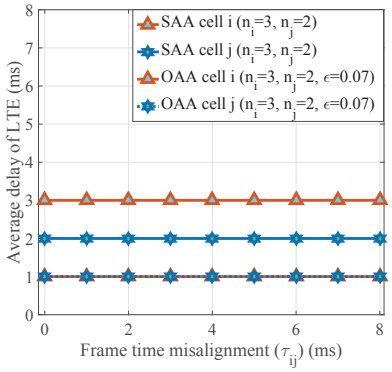

Fig. 5: Delay of LTE network vs. frame time misalignment (τ_{ij}) (Problem 1).

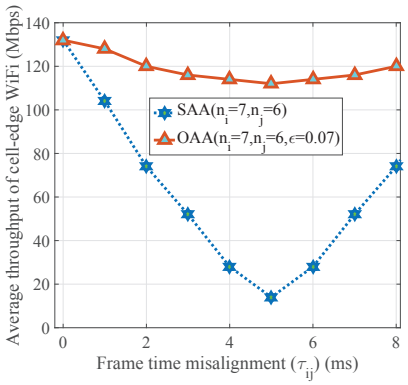

Fig. 6: Average throughput of cell-edge WiFi network vs. frame time misalignment (τ_{ij}) (Problem 2).

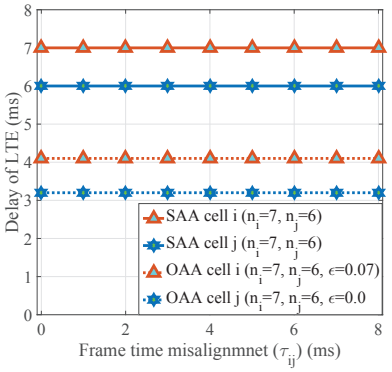

Fig. 7: Delay of LTE network vs. frame time misalignment (τ_{ij}) (Problem 2).

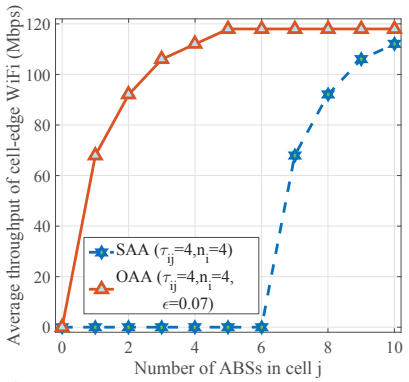

Fig. 8: Average throughput of cell-edge WiFi network vs. number of ABSs in cell j (Problem 1).

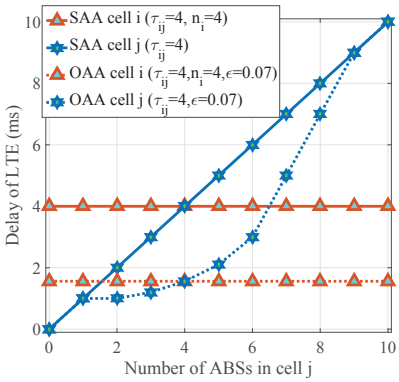

Fig. 9: Delay of LTE network vs. number of ABSs in cell j (Problem 1).

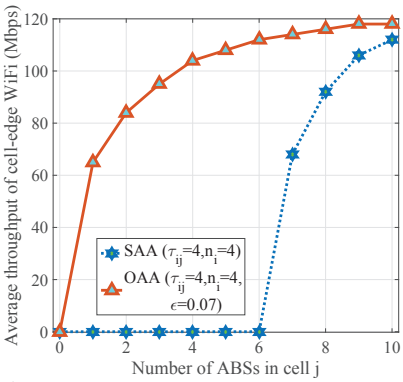

Fig. 10: Average throughput of cell-edge WiFi network vs. number of ABSs in cell j (Problem 2).

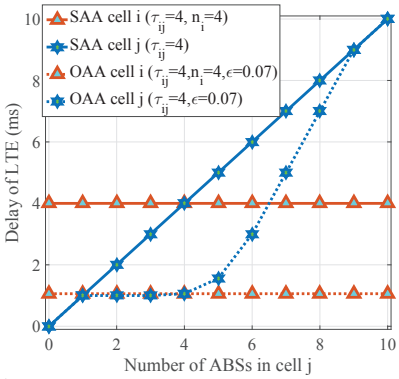

Fig. 11: Delay of LTE network vs. number of ABSs in cell j (Problem 2).

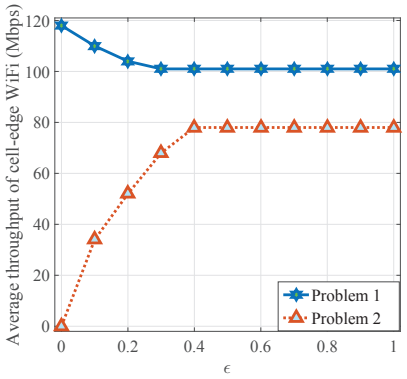

Fig. 12: Average throughput of cell-edge WiFi network vs. ϵ.

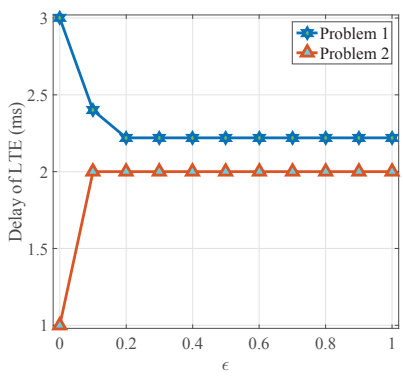

Fig. 13: Delay of LTE network vs. ϵ.

to 8 ms while keeping the other parameters fixed, $n_i = 3$, $n_j = 2$, and $\epsilon = 0.07$. We considered a small number of ABSs to create a challenging scenario for having overlapped ABSs between two cells. As we can clearly see in Figure 4, when τ_{ij} increases, the average throughput of cell-edge WiFi network for SAA scheme decreases rapidly and goes to zero when $\tau_{ij} \geq 6$ ms, whereas, our OAA scheme shows an almost constant curve. Also, in Figure 5, we can see that the delay of the LTE network is decreased to almost 1 ms for both cells. These signify the success of the optimal solution of Problem 1. Similarly, we study the performance of the optimal solution of Problem 2 in Figures 6 and 7 by varying τ_{ij} from 0 ms to 8 ms. To analyze the performance of the LTE network delay, now higher values for n_i and n_j (i.e. $n_i = 7$, $n_j = 6$, and $\epsilon = 0.07$) are considered, because this makes the scenario of having no consecutive ABSs more challenging. In Figure 7,

we can see that the delay of the LTE network decreases from 7 ms (SAA scheme) to 3 ms (OAA scheme) for cell i and from 5 ms (SAA scheme) to 1 ms (OAA scheme) for cell j. This clearly shows the efficiency of our scheme. Also, in Figure 6, we see that our scheme shows significantly better performance in terms of the average throughput of the WiFi network. It is worth mentioning that for this higher values of n_i and n_j, at $\tau_{ij} \geq 5$, for SAA scheme, the ABSs of cell j starts to overlap with the ABSs of the next frame of cell i. This causes certain improvement in the WiFi network performance of SAA scheme at $\tau_{ij} \geq 5$.

In Figures 8 and 9, we analyze the performance of the optimal solution of Problem 1 by varying the number of ABSs in cell j while keeping the other parameters fixed, $n_i = 4$, $\tau_{ij} = 4$, and $\epsilon = 0.07$. In Figure 8, we see that SAA scheme shows zero throughput for cell-edge WiFi network until the number of ABSs in cell j, i.e. $n_j \geq 7$. Whereas, our scheme exhibits sharp rise in WiFi throughput with increasing n_j. In Figure 9, we see that SAA scheme shows linear increase in LTE delay for cell j and a constant 4 ms delay for cell i. But, in our OAA scheme, the delay of LTE for cell i decreases to almost 2 ms. For cell j, when $n_j \leq 5$ our scheme shows a delay of LTE less than 2 ms but experiences a sharp rise for $n_j \geq 5$. The reason for this is when $n_j = 5$, there is only one ABS location set exists which does not have any consecutive ABS i.e. $\{1, 3, 5, 7, 9\}$. When $n_i \geq 6$, after the $1^{st}, 3^{rd}, 5^{th}, 7^{th}$ and 9^{th} subframe locations are chosen, any further entry would cause 3 consecutive ABSs with 3 ms delay. Similarly another entry would cause 5 ms delay and so on.

In Figures 10 and 11, the performance of the optimal solution of Problem 2 is studied by varying n_j while keeping the other parameters fixed, $n_i = 4$, $\tau_{ij} = 4$, and $\epsilon = 0.07$. As we can see in Figure 11, the delay of the LTE network is 1 ms for cell j when $n_j \leq 5$. After that, the delay increases rapidly for the same reason discussed before. Cell i also shows a smaller delay of almost 1 ms. Further, in Figure 10, we can see that our scheme again outperforms SAA in terms of the throughput of cell-edge WiFi users.

Finally, in Figures 12 and 13 we study the impact of ϵ on the optimal solutions of Problems 1 and 2 while keeping the other parameters fixed $n_i = 5$, $n_j = 5$, and $\tau_{ij} = 7$. For $n_i = n_j = 5$, at $\epsilon = 0$, in Problem 1, while maximizing $\mathcal{R}\left(x_s, n_i, \tilde{n}_j, \tilde{\tau}_{ij}\right)$, i and j choose that optimal grid structure which does not produce one of ABS location sets as $\{1, 3, 5, 7, 9\}$. This results in 3 ms delay for both cells. Then, as ϵ increases from 0 to 1, that particular grid structure is selected which reduces the probability of consecutive ABSs resulting less delay (i.e. around 2.3 ms delay) for LTE. Similarly, for Problem 2, while minimizing $\mathcal{D}\left(x_s, n_i, \tilde{n}_j, \tilde{\tau}_{ij}\right)$, for $\epsilon = 0$ ABS location sets as $\{1, 3, 5, 7, 9\}$ is chosen which results 0 throughput for cell-edge WiFi network for this particular set of parameters. After that, as ϵ increases, average throughput of cell-edge WiFi also increases compromising a delay of 2 ms for LTE.

VI. Conclusion

In this paper, we proposed an optimal distributed ABS allocation scheme inspired from grid quorum systems. The proposed scheme optimally allocates a given number of ABSs over an LTE frame to provide QoS guarantees for LTE and WiFi network. The numerical analysis shows that our optimal ABS allocation scheme outperforms the sequential ABS allocation scheme under different scenarios. In future, we would like to extend our work for the cell-edge WiFi users lying in the overlapping region of three different cells.

References

[1] A. T. Saeed, A. Esmailpour, and N. Nasser, "Performance analysis for the QoS support in LTE and WiFi," in *Proceedings of the IEEE WCNC Workshops*, 2016, pp. 289–295.

[2] Z. Zhou, F. Teng, J. Liu, and W. Xiao, "Performance evaluation for coexistence of LTE and WiFi," in *Proceedings of the IEEE ICNC Conference*, 2016, pp. 1–6.

[3] Y. Song, K. W. Sung, and Y. Han, "Coexistence of Wi-Fi and cellular with listen-before-talk in unlicensed spectrum," *IEEE Communications Letters*, vol. 20, no. 1, pp. 161–164, 2016.

[4] J. Wang, L. Liu, L. Wang, H. Harada, and H. Jiang, "Downlink HARQ enhancement for listen-before-talk based LTE in unlicensed spectrum," in *Proceedings of the IEEE WCNC Conference*, 2016, pp. 1–6.

[5] H. Wang, M. Kuusela, C. Rosa, and A. Sorri, "Enabling frequency reuse for licensed-assisted access with listen-before-talk in unlicensed bands," in *Proceedings of the IEEE Vehicular Technology Conference (VTC Spring)*, 2016, pp. 1–5.

[6] F. S. Chaves, E. P. Almeida, R. D. Vieira, A. M. Cavalcante, F. M. Abinader, S. Choudhury, and K. Doppler, "LTE UL power control for the improvement of LTE/Wi-Fi coexistence," in *Proceedings of the IEEE Vehicular Technology Conference (VTC Fall)*, 2013, pp. 201–207.

[7] A. Galanopoulos, F. Foukalas, and T. A. Tsiftsis, "Efficient coexistence of LTE with WiFi in the licensed and unlicensed spectrum aggregation," *IEEE Transactions on Cognitive Communications and Networking*, vol. 2, no. 2, pp. 129–140, 2016.

[8] Q. Chen, G. Yu, and Z. Ding, "Optimizing unlicensed spectrum sharing for LTE-U and WiFi network coexistence," *IEEE Journal on Selected Areas in Communications*, vol. 55, no. 3, pp. 20–33, 2016.

[9] J. Xiao and J. Zheng, "An adaptive channel access mechanism for LTE-U and WiFi coexistence in an unlicensed spectrum," in *Proceedings of the IEEE ICC Conference*, 2016, pp. 1–6.

[10] "Extending LTE advanced to unlicensed spectrum." Qualcomm, 2013.

[11] O. Sallent, J. Pérez-Romero, R. Ferrús, and R. Agustí, "Learning-based coexistence for LTE operation in unlicensed bands," in *Proceedings of the IEEE ICC Workshop*, 2015, pp. 2307–2313.

[12] M. J. Abdel-Rahman, M. AbdelRaheem, A. MacKenzie, K. Cardoso, and M. Krunz, "On the orchestration of robust virtual LTE-U networks from hybrid half/full-duplex Wi-Fi APs," in *Proceedings of the IEEE WCNC Conference*, 2016, pp. 44–50.

[13] E. Almeida, A. M. Cavalcante, R. C. Paiva, F. S. Chaves, F. M. Abinader, R. D. Vieira, S. Choudhury, E. Tuomaala, and K. Doppler, "Enabling LTE/WiFi coexistence by LTE blank subframe allocation," in *Proceedings of the IEEE ICC Conference*, 2013, pp. 5083–5088.

[14] M. Sriyananda, I. Parvez, I. Güvene, M. Bennis, and A. I. Sarwat, "Multi-armed bandit for LTE-U and WiFi coexistence in unlicensed bands," in *Proceedings of the IEEE WCNC Conference*, 2016, pp. 1–6.

[15] N. Rupasinghe and İ. Güvenç, "Reinforcement learning for licensed-assisted access of LTE in the unlicensed spectrum," in *Proceedings of the IEEE WCNC Conference*, 2015, pp. 1279–1284.

[16] S. Han, Y.-C. Liang, Q. Chen, and B.-H. Soong, "Licensed-assisted access for LTE in unlicensed spectrum: A MAC protocol design," in *Proceedings of the IEEE ICC Conference*, 2016, pp. 21–27.

[17] H. Zhang, X. Chu, W. Guo, and S. Wang, "Coexistence of Wi-Fi and heterogeneous small cell networks sharing unlicensed spectrum," *IEEE Communications Magazine*, vol. 53, no. 3, pp. 158–164, 2015.

[18] A. Checco and D. J. Leith, "Proportional fairness in 802.11 wireless LANs," *IEEE Communications Letters*, vol. 15, no. 8, pp. 807–809, 2011.